Clinical Cancer Research

PQR309 Is a Novel Dual PI3K/mTOR Inhibitor with Preclinical Antitumor Activity in Lymphomas as a Single Agent and in Combination Therapy

Chiara Tarantelli[1], Eugenio Gaudio[1], Alberto J. Arribas[1], Ivo Kwee[1,2,3], Petra Hillmann[4], Andrea Rinaldi[1], Luciano Cascione[1,5], Filippo Spriano[1], Elena Bernasconi[1], Francesca Guidetti[1], Laura Carrassa[6], Roberta Bordone Pittau[5], Florent Beaufils[4,7], Reto Ritschard[8], Denise Rageot[4,7], Alexander Sele[7], Barbara Dossena[9], Francesca Maria Rossi[10], Antonella Zucchetto[10], Monica Taborelli[9], Valter Gattei[10], Davide Rossi[1,5], Anastasios Stathis[5], Georg Stussi[5], Massimo Broggini[6], Matthias P. Wymann[7], Andreas Wicki[8], Emanuele Zucca[5], Vladimir Cmiljanovic[4], Doriano Fabbro[4], and Francesco Bertoni[1,5]

Abstract

Purpose: Activation of the PI3K/mTOR signaling pathway is recurrent in different lymphoma types, and pharmacologic inhibition of the PI3K/mTOR pathway has shown activity in lymphoma patients. Here, we extensively characterized the *in vitro* and *in vivo* activity and the mechanism of action of PQR309 (bimiralisib), a novel oral selective dual PI3K/mTOR inhibitor under clinical evaluation, in preclinical lymphoma models.

Experimental Design: This study included preclinical *in vitro* activity screening on a large panel of cell lines, both as single agent and in combination, validation experiments on *in vivo* models and primary cells, proteomics and gene-expression profiling, and comparison with other signaling inhibitors.

Results: PQR309 had *in vitro* antilymphoma activity as single agent and in combination with venetoclax, panobinostat, ibrutinib, lenalidomide, ARV-825, marizomib, and rituximab. Sensitivity to PQR309 was associated with specific baseline gene-expression features, such as high expression of transcripts coding for the BCR pathway. Combining proteomics and RNA profiling, we identified the different contribution of PQR309-induced protein phosphorylation and gene expression changes to the drug mechanism of action. Gene-expression signatures induced by PQR309 and by other signaling inhibitors largely overlapped. PQR309 showed activity in cells with primary or secondary resistance to idelalisib.

Conclusions: On the basis of these results, PQR309 appeared as a novel and promising compound that is worth developing in the lymphoma setting. *Clin Cancer Res; 24(1); 120–9. ©2017 AACR.*

Introduction

PI3Ks are enzymes belonging to PI3K/AKT/mTOR signaling pathways with a central role in the regulation of cell metabolism, proliferation, and survival (1, 2). Class IA PI3Ks include heterodimers of p110 catalytic subunit and p85 regulatory subunit (1–3). The class IA catalytic subunit isoforms are encoded by the genes *PIK3CA*, *PIK3CB*, and *PIK3CD* (1–3): p110α (PI3Kα), p110β (PI3Kβ), and p110δ (PI3Kδ), respectively. These isoforms can associate with any of five regulatory isoforms, p85α and its splicing variants p55α and p50α (*PIK3R1*), p85β (*PIK3R2*), and p55γ (*PIK3R3*), generally called p85 type regulatory subunits (1–3). Class IB PI3Ks are heterodimers of a p110γ (PI3Kγ) catalytic subunit (*PIK3CG*) with regulatory isoforms p101 (*PIK3R5*) or p87 (*PIK3R6*). While PI3Kα and PI3Kβ are ubiquitously expressed, PI3Kδ, and PI3Kγ are largely restricted to leukocytes (1–3).

PI3K/AKT/mTOR signaling pathway activation is common in lymphomas. Examples are mutations or gains of *PIK3CA* in diffuse large B-cell lymphoma (DLBCL), mantle cell lymphomas (MCL), and chronic lymphocytic leukemias (CLLs; refs. 4, 5), inactivation or low expression of *PTEN* in DLBCL, follicular lymphomas (FL), MCL and CLL (5–8).

The approval by regulatory authorities of the mTOR inhibitor temsirolimus for MCL (9) and of the PI3Kδ inhibitor idelalisib for FL and CLL (10, 11) strongly encouraged further development of compounds targeting PI3K complex and/or mTOR (12–15). Dual

[1]Università della Svizzera Italiana (USI), Institute of Oncology Research (IOR), Bellinzona, Switzerland. [2]Dalle Molle Institute for Artificial Intelligence (IDSIA), Manno, Switzerland. [3]Swiss Institute of Bioinformatics (SIB), Lausanne, Switzerland. [4]PIQUR Therapeutics AG, Basel, Switzerland. [5]Oncology Institute of Southern Switzerland (IOSI), Bellinzona, Switzerland. [6]IRCCS-Istituto di Ricerche Farmacologiche Mario Negri, Milan, Italy. [7]Department of Biomedicine, University of Basel, Basel, Switzerland. [8]Department of Oncology, University Hospital Basel, Basel, Switzerland. [9]Cytogenetics Laboratory, Ente Ospedaliero Cantonale, Bellinzona, Switzerland. [10]Clinical and Experimental Onco-Hematology Unit, IRCCS-Centro di Riferimento Oncologico, Aviano, Italy.

Note: Supplementary data for this article are available at Clinical Cancer Research Online (http://clincancerres.aacrjournals.org/).

C. Tarantelli and E. Gaudio contributed equally to this article.

Corresponding Author: Francesco Bertoni, Institute of Oncology Research, via Vela 6, Bellinzona 6500, Switzerland. Phone: 41-91-820-0367; Fax: 41-91-820-0397; E-mail: frbertoni@mac.com

doi: 10.1158/1078-0432.CCR-17-1041

Translational Relevance

Targeting PI3K and mTOR is an important therapeutic opportunity to improve the outcome of individuals affected by lymphomas. PQR309 is a novel brain-penetrant dual PI3K/mTOR inhibitor with *in vitro* and *in vivo* antilymphoma activity as single agent and in combination, and importantly, can overcome both primary and acquired resistance to idelalisib, the most frequently used PI3K inhibitor in the clinical setting. The presented highly overlapping changes in the lymphoma transcriptome observed by a direct comparison of the gene expression changes induced by PQR309 and other different BCR inhibitors may have implications in the design of novel combination schemes.

PI3K/mTOR inhibitors with strong activity toward all p110 isoforms and mTOR combine multiple therapeutic efficacies in a single molecule (3). Pan PI3K inhibitors are expected to reduce the risk of drug resistance that might occur in case of treatment with compounds targeting a single p110 isoform (16) and, together with mTOR inhibition, could prevent feedback loop of AKT activation following mTOR inhibition (17). PQR309 (bimiralisib) is a novel orally bioavailable selective dual PI3K/mTOR inhibitor (18, 19), and, differently from most PI3K and mTOR inhibitors (20), able to cross the brain blood barrier (18). Here, we present the preclinical characterization of PQR309 as single agent and in combination with several other agents in pre-clinical models of lymphomas. Proteomic and/or genomic approaches were also used with the aim to uncover the mechanism of action of the compound in parallel with other targeted signaling inhibitors.

Materials and Methods

Cell lines

A total of 49 human established lymphoma cell lines were used: seven (RI-1, HBL-1, TMD8, U2932, SU-DHL-2, OCI-LY-3, OCI-LY-10) from activated B-cell–like DLBCL (ABC DLBCL), 18 (Pfeiffer, OCI-LY-1, OCI-LY-2, OCI-LY-7, OCI-LY-8, OCI-LY-18, OCI-LY-19, KARPAS422, SU-DHL-4, SU-DHL-6, SU-DHL-7, SU-DHL-10, FARAGE, VAL, WSU-DLCL2, TOLEDO, RCK8, DOHH2) from germinal center B-cell (GCB) DLBCL, 10 (GRANTA-519, JEKO1, JVM-2, MAVER-1, MINO, REC-1, SP-49, SP-53, UPN-1 and Z-138) from MCL, three (KARPAS1718, VL51, SSK41) from splenic marginal zone lymphoma (SMZL), two (MEC-1, PCL-12) from CLL, four (L-1236, KM-H2, L428 and AM-HLH) from Hodgkin lymphoma and five (Ki-JK, KARPAS299, L-82, SU-DHL-1, FEPD) from anaplastic large cell lymphoma (ALCL). All media were supplemented with FBS (10%), penicillin–streptomycin–neomycin (~5,000 U penicillin, 5 mg streptomycin and 10 mg neomycin/mL, Sigma), and L-glutamine (1%).

Fluorescence *in situ* hybridization for *MYC* translocation

Cells spotted onto glass microscope slides were washed, dehydrated in an ethanol series. Ten μL of FISH probe mixture [XL t(8;14) Dual Fusion Probe, D-5008-100-OG, MetaSystems Probes GmbH, Germany] were spotted onto the cell sample, slides were denatured at 75°C for 2 minutes, hybridized at 37°C overnight, washed and dehydrated with an ethanol series, stained with 4′-6′-diamidino-2-phenylindol (DAPI) and analyzed with a BX61 microscope (Olympus Italia, Milan, Italy) using the Cytovision Imaging System (Applied Imaging).

Compounds

PQR309 and apitolisib (GDC0980) were provided by Piqur Therapeutics, venetoclax, ibrutinib, idelalisib, duvelisib, AZD1208, lenalidomide, panobinostat were purchased from Selleckchem, ARV-825 and metformin from MedChem, marizomib from AdooQ and rituximab from Roche.

Primary cells

Peripheral blood was obtained from patients diagnosed with CLL according to standard criteria. All patients signed informed consent (BASEC 2016-00511, CE 3051). CLL cells were isolated by Ficoll density-gradient centrifugation and CLL cells (5×10^5 cells/mL) were cultured for 48 hours, and the percentage of viable and apoptotic CLL cells [Annexin V positive/7-Aminoactinomycin D (7AAD) negative and Annexin V positive/7AAD positive] was determined by double staining the cells with Annexin V–FITC/7AAD.

In vitro antitumor activity

The antiproliferative activity in 384-well plates (21), the IC_{50} values estimate (22) and drug combinations screening (23) were performed as previously described. Combinations were defined: synergistic if the Chou-Talalay Combination Index (CI) was <0.9; additive if CI between 0.9 and 1.1; antagonistic if CI > 1.1 (24). Apoptosis and cell cycle were evaluated as previously reported (22). Apoptosis induction was defined in the presence of a 2-fold or higher increase in comparison with DMSO-treated cells.

In vivo experiments

Three *in vivo* experiments were performed. The first two explored PQR309 as single agent and in combination with ibrutinib in the RI-1 cell line or venetoclax in the SU-DHL-6 cell line. For these, NOD-Scid (NOD.CB17-*Prkdcscid*/NCrHsd) mice were subcutaneously inoculated with the RI-1 cell line (1×10^7 cells in 0.1 ml of PBS, 1:1 Matrigel) or with the SU-DHL-6 cell line (5×10^6 cells in 100 μL of PBS, 1:1 Matrigel). Mice maintenance and animal experiments were performed under the Guide of animal care and use (NCR 2011) and under the Chinese National Standard (GB14925-2010; Crown Bioscience Inc.). For the third experiment, exploring PQR309 as single agent and in combination with venetoclax in the RI-1 cell line, NOD-Scid (NOD.CB17-*Prkdcscid*/NCrHsd) mice (Harlan Laboratories) were subcutaneously inoculated with the cell line (1×10^7 cells in 0.1 mL of PBS). Mice maintenance and animal experiments were performed under institutional guidelines established for the Animal Facility and with study protocols approved by the local Cantonal Veterinary Authority. Treatments were started with tumors of approximately 150 mm^3 volume. Tumor size was measured using a digital caliper [tumor volume (mm^3) = $D \times d^2/2$]. Differences in tumor volumes were calculated using the Wilcoxon rank-sum test (Stata/SE 12.1 for Mac, Stata Corporation). The *P* value for significance was <0.05.

Western blotting analysis

Protein extraction, separation and immunoblotting were performed as previously described (25). The following antibodies were used: anti-Vinculin (V9131, Sigma-Aldrich), anti-AKT (9272, Cell Signaling Technology), anti–phospho-AKT (Ser473;

4060, Cell Signaling Technology), and anti-phospho-p70S6K (Thr389; 9205, Cell Signaling Technology).

PhosphoFlow cytometry

For phosphoprotein expression analysis, parental and idelalisib-resistant KARPAS1718 and VL51 cells (5×10^5 per experimental condition) were overnight treated with 1 μmol/L of idelalisib or PQR309 or with DMSO, and stimulated or not for 15 minutes with 10 μg/mL F(ab)2 anti-IgM (109.006.129, Jackson Immunoresearch). Cells were then fixed with Fix Buffer I (BD Biosciences), and permeabilized with 90% ice-cold methanol. Cells were labelled with p-mTOR (pS2448)-Alexa-647 (564242, BD Bioscience) and analyzed on a FACS Fortessa flow cytometer using FACS DIVA software (BD Biosciences).

The FlowCellect PI3K Activation Dual Detection Kit (Merck Millipore) was used according to the manufacturer's instructions. Flow-cytometry analysis was carried out with a FACSCantoII instruments (BD Biosciences) and data were analyzed using BD FACSDiva v8.0.1 software (BD Biosciences). To avoid counting false positive cells, cells stained with anti–AKT-Alexa Fluor 488 only were used as negative controls.

Antibody array

The protein lysate prepared as previously described (25), was incubated with the PathScan AKT Signaling Antibody Array Kit (Cell Signaling Technology) following the manufacturer's instructions. A standard curve was prepared using protein lysate from MCF7 cell line induced for 1 hour with 20 ng/μL IGF-1. Image was captured and analyzed with Image Studio Ver4.0 (LI-COR Biotechnology). Scanning properties were: high quality, 21 μm/px, 0.0-mm interval and intensity 2.0. The image was analyzed with a grid array composed of 8×2 arrays, each consisting of 6 rows and 6 columns; the size of each case was 1,005 pixels and the background was adjusted by selecting the spot at the right bottom. All data were exported in an Excel file.

Reverse phase protein array

Cells were washed in PBS and lysed with the RIPA Lysis and Extraction Buffer (Thermo Fisher Scientific) supplemented with proteasome and phosphatase inhibitors (Thermo Fisher Scientific). Cell lysates were spotted onto glass slides at Carna Biosciences and immunostaining was performed with 180 antibodies, each one on an individual slide (list of antibodies in Supplementary Table S1). Signals were measured as fluorescence of the fluorophore-labeled secondary antibodies and were normalized with gamma-tubulin.

Mass spectrometry

Cells were washed in PBS and lysed with the Biognosys' Lysis Buffer adding benzonase nuclease (Biognosys AG). Protein concentration was determined using the mBCA assay (Pierce). Proteins (1 mg/sample) were reduced, samples were alkylated, diluted, digested, desalted, and dried down following a Biognosys proprietary protocol. Phosphopeptides were enriched with TiO2 and cleaned up with MicroSpin C18 columns (The Nest Group, Inc.), dried down and resuspended in Biognosys LC solvent (20 μL). The peptide concentration was determined using mBCA assay (Pierce). Solvents for liquid chromatography (LC) were: A, 1% acetonitrile in water with 0.1% formic acid; B, 3% water in acetonitrile with 0.1% formic acid. A consistent amount of 2 μg of protein was injected.

The LC gradient was 1% to 38% solvent B in 120 minutes followed by 35% to 100%B in 2 minutes and 100% B for 8 minutes (total gradient length was 130 minutes). All mass spectrometric analyses were carried out on a Q Exactive mass spectrometer at Biognosys. For shotgun analyses a modified TOP12 method was used (26). For Hyper Reaction Monitoring (HRM) a Data-independent acquisition (DIA) method with one full range survey scan and 19 DIA window was used, the gradient length was 130 minutes. The LC-MS/MS (shotgun) mass spectrometric data were analyzed using the MaxQuant 1.5.1.2 software (27), the FDR on peptide and protein level was set to 1%. Uniprot human FASTA sequences (no isoforms) database was used for the search engine (state 11.12.2014). Phospho modifications (STY) and two missed trypsin cleavages were allowed. HRM mass spectrometric data were analyzed using Spectronaut 7.0 software (Biognosys). The FDR on peptide level was set to 1%, data was filtered using row-based extraction. The assay library generated in this project was used for the targeted analysis approach. Quality control was performed by a control sample (human blood plasma) measured before and after profiling MS measurements in shotgun proteomics, the analysis of the two control measurements revealed that the performance stayed constant over the time of acquisition. The HRM measurements analyzed with Spectronaut were normalized using local regression normalization. Probes (42 out of 5,028) with a detection q value more than 0.01 in more than half of the cases were removed from further analysis.

Gene expression analysis

Gene-expression profiling (GEP) was done using the HumanHT-12 v4 Expression BeadChip (Illumina), as previously described (28). The transcripts interrogated by probes were updated with the new reference genome database via the Re-Annotator software (29). Raw intensities were normalized by using quantile method.

For targeted RNA-Seq, cell lines were lysed, and then processed using the HTG EdgeSeq Oncology Biomarker panel (HTG Molecular Diagnostics, Inc.). The labeled samples pooled, cleaned, and sequenced on an Illumina NextSeq using a High Output, 75-cycle, v2 kit with two index reads, as previously described (30).

All GEP data are available at the National Center for Biotechnology Information (NCBI) Gene Expression Omnibus (GEO; http://www.ncbi.nlm.nih.gov/geo) database: GSE64820 (23), GSE94669 and GSE103934 for baseline and GSE94670 for treated samples.

Data mining

For exploratory proteomic studies, differences in phosphorylation were defined as statistically significant if log ratio was $> |0.3|$ with a $P < 0.05$ using the empirical Bayes (paired) moderated t test as implemented in the LIMMA R-package (31). Functional annotation was performed using the Gene Set Enrichment Analysis (GSEA) on-line tool for overlap analysis using the Molecular Signatures Database (MSigDB) 5.2 (32).

For GEP comparisons between cell lines exposed to compounds or controls, probes presenting an FDR, controlled by the Benjamini-Hochberg algorithm, <0.05 and a log ratio $> |0.3|$ were considered differentially expressed using the empirical Bayes (paired) moderated t test as implemented in the LIMMA R-package (31). Gene sets enrichment was defined with GSEA (32)

on pre-ranked lists using the MSigDB 5.2 (32) and the SignatureDB collection (33) applying a threshold based on FDR < 0.1.

For exploratory analyses performed on baseline gene expression profiles of cell lines with different degree of sensitivity to compounds, Illumina probes presenting a $P < 0.05$ and a log ratio > |0.3| were defined differentially expressed using a non-parametric Wilcoxon test on the CARMAweb 1.6 (34). Gene sets enrichment was defined with GSEA (32) applying a threshold based on FDR < 0.1. For data obtained with the HTG EdgeSeq Oncology Biomarker panel, FASTQ data were aligned and RNA expression was reported as counts per probe per sample using the HTG EdgeSeq parser software: Genes were defined differentially expressed when $P \geq 0.9$ (where P is the probability to be differentially expressed) after NOISeq non-parametric test (35).

Results

The dual PI3K/mTOR inhibitor PQR309 has *in vitro* antitumor activity in lymphoma

The novel dual PI3K/mTOR inhibitor PQR309 was evaluated in 49 lymphoma cell lines, exposed to increasing doses of the molecule (72 hours), showing *in vitro* activity in most of them tested with a median IC_{50} value of 233 nmol/L (95% CI, 174–324 nmol/L; Fig. 1A). The arrest in proliferation was mainly due to cell cycle arrest with a block in G_1 (Fig. 1C and D) rather than to apoptosis, limited to only 2/7 cell lines (Fig. 1B). PQR309 was more active in B-cell lymphoma cell lines (DLBCL, MCL, CLL, and SMZL) than in the T-cell derived ALCL ($P = 0.028$). There were no differences in terms of sensitivity between activated B-cell like (ABC; $n = 7$) and germinal center B-cell (GCB; $n = 18$) DLBCL subtypes, between *de novo* DLBCL ($n = 9$) and DLBCL derived from transformed FL ($n = 12$), or based upon *TP53* [active ($n = 6$) vs. inactive ($n = 25$)], *MYC* [translocation or genomic amplification ($n = 12$) vs. normal ($n = 4$)], or *BCL2* [translocation or genomic amplification ($n = 14$) vs. normal ($n = 3$)] genes status (Supplementary Table S2).

PQR309 presented a highly-correlated pattern of antiproliferative activity with another, non-brain penetrant, dual PI3K/mTOR inhibitor, apitolisib (GDC-0980; ref. 36; $R = 0.94$, $P < 0.0001$; Supplementary Fig. S1).

PQR309-containing combinations are synergistic in B-cell lymphoma cell lines

The antitumor activity of PQR309 was evaluated in combination with compounds already in the clinics for lymphoma patients or targeting important biologic pathways, often achieving a benefit (Supplementary Table S2).

PQR309 combination with the BTK inhibitor ibrutinib resulted in synergism in 10/11 cell lines (6/7 ABC-DLBCL, 4/4 MCL), a benefit that was confirmed using an ABC-DLBCL (RI-1) xenograft model (schedules in SI; Supplementary Fig. S2A).

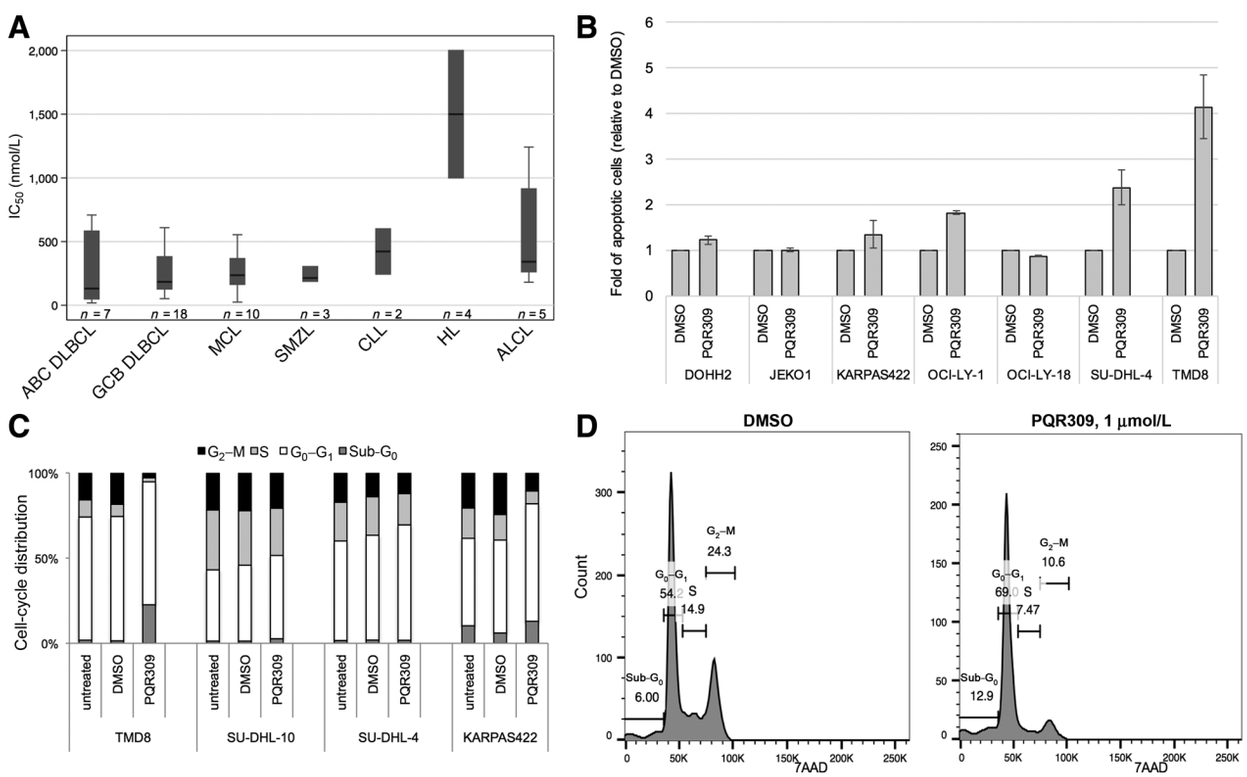

Figure 1.

PQR309 has *in vitro* antitumor activity in lymphoma. **A,** IC_{50} values (nmol/L) calculated performing MTT assay in lymphoma cell lines after PQR309 (72 hours). In each box plot, the line in the middle of the box represents the median and the box extends from the 25th to the 75th percentile (interquartile range, IQ); the whiskers extend to the upper and lower adjacent values (i.e., ±1.5 IQ); outside values have been omitted from the figure. **B,** Induction of apoptosis after PQR309 (500 nmol/L) or DMSO (72 hours). Apoptosis induction was determined when more than 2-fold. **C,** Cell-cycle distribution after PQR309 (1 μmol/L) or DMSO (72 hours). **D,** Representative histogram of cell-cycle distribution in KARPAS422 cells treated with PQR309 (1 μmol/L) or DMSO (72 hours).

Synergism/additivity was obtained in 10/12 cell lines exposed to PQR309 and the BCL2 inhibitor venetoclax. The beneficial effect was confirmed in terms of increased cell death induction in three CLL primary cells and in SU-DHL-6 cell line (Supplementary Fig. S3A–S3C). Furthermore, the combination with venetoclax was also assessed in both GCB- (SU-DHL-6) and ABC-DLBCL (RI-1) xenograft models (schedules in SI) resulting in a significantly stronger antitumor activity than single agents (Supplementary Fig. S2B and S2C).

The combination of PQR309 with the HDAC inhibitor panobinostat was beneficial in 5/6 cell lines (four synergisms, one additive effect), also confirmed in the CLL primary cells and in SU-DHL-6 cell line (Supplementary Fig. S3A–S3C). Finally, benefit was observed combining PQR309 with the PROTAC BET inhibitor ARV-825 (6/8 cell lines; four synergisms, two additive effects), the immunomodulatory lenalidomide (3/4; all synergisms), the anti-CD20 monoclonal antibody rituximab (2/5; both synergisms), and with the proteasome inhibitor marizomib (1/4; synergism).

Baseline features are associated with sensitivity to PQR309

To identify genetic or biologic features associated with different degree of sensitivity to PQR309 we compared the baseline gene expression profiles of B-cell lymphoma cell lines with a very high sensitivity (IC_{50} < 200 nmol/L, $n = 20$) versus cell lines with a lower sensitivity to the compound (IC_{50} > 400 nmol/L, $n = 7$). Transcripts preferentially expressed in sensitive cell lines were significantly enriched of genes involved in BCR pathway/signaling and BLIMP1 targets (Supplementary Fig. S4A; Supplementary Table S3A). Transcripts associated with less sensitive cell lines were enriched of members of proteasome pathway, response to unfolded proteins, MYC targets, XBP1 targets, genes downregulated by mTOR inhibitors and genes involved in oxidative phosphorylation (Supplementary Fig. S4B; Supplementary Table S3B). Among the genes coding for the PI3K complexes, *PIK3R1*, *PIK3R2*, *PIK3CD*, were positively correlated with high sensitivity to PQR309, whereas *PIK3CG*, *PIK3CA*, and *PIK3R6* were associated with low sensitivity (Supplementary Table S3C). Supplementary Table S3D contains the differentially expressed genes. Finally, we also analyzed the gene-expression profile related to cell lines with different degrees of sensitivity to PQR309 using a targeted RNA-Seq-based technology, which can be readily applied to formalin-fixed paraffin-embedded specimens (ref. 30; Supplementary Table S3E). Thirteen genes (*ACTR2*, *ALCAM*, *CD52*, *CDK1*, *EVL*, *LIPA*, *MGEA5*, *NFATC1*, *PRKAR1A*, *REL*, *RHOA*, *VHL*, and *ZFP36L1*) were found commonly upregulated in sensitive cell lines both with the Illumina arrays and with the HTG EdgeSeq Oncology Biomarker panel (Supplementary Table S3F).

PQR309 is active in lymphoma cell lines with primary and secondary resistance to idelalisib

We exposed all the cell lines tested for sensitivity to PQR309 also to the PI3Kδ inhibitor idelalisib to identify cases with a primary resistance to the latter drug but still sensitive to the dual PI3K/mTOR inhibitor. The median IC_{50} value for idelalisib was 2.98 μmol/L (738 nmol/L–10.3 μmol/L; Supplementary Fig. S5A), higher than what seen for PQR309. Its pattern of activity correlated with PQR309 ($R = 0.66$, $P < 0.0001$; Supplementary Fig. S5B), although at a lesser extent than what was seen between the 2 dual PI3K/mTOR inhibitors (Supplementary Fig. S1B). Similar to PQR309, idelalisib was more active in the B-cell than in T-cell ALCL cell lines ($P = 0.021$).

We compared the transcriptome of 25 dual sensitive B-cells (IC_{50} < 5 μmol/L for idelalisib, equal to clinically achievable concentration (37), IC_{50} < 400 nmol/L for PQR309) versus seven sensitive only to PQR309(Supplementary Table S4). Transcripts highly expressed in the dual sensitive cell lines were enriched of genes involved in interferon signaling, PI3K/AKT/mTOR, cytokine and chemokine signaling (Supplementary Table S4A and S4C). Conversely, the discordant cell lines expressed transcripts enriched of genes involved in cell cycle, amino acids metabolism and E2F targets (Supplementary Table S4B and S4C). Regarding the genes coding for the PI3K complexes, *PIK3CD*, *PIK3R2*, *PIK3R6*, *PIK3R5* were positively correlated with the dual sensitive phenotype, whereas *PIK3CA*, *PIK3CG* and *PIK3CB*, *PIK3R1*, *PIK3R3* were associated with the discordant phenotype (Supplementary Table S4D).

We then took advantage of novel models of stable secondary resistance to idelalisib recently developed in our laboratory exposing two SMZL cell lines (VL51, KARPAS1718) to continuous IC_{90} concentrations of the PI3Kδ inhibitor (38). Despite increases in the IC_{50} values of over five times for idelalisib (Fig. 2A and B), both the idelalisib-resistant and parental cells presented the same sensitivity to PQR309 (Fig. 2C and D). PQR309 was able to reduce p-mTOR in both parental and idelalisib-resistant KARPAS1718 stimulated or unstimulated with anti-IgM ($P < 0.05$; Fig. 2E), whereas idelalisib weakly decreased MTOR-Ser2448 phosphorylation levels in resistant cells ($P < 0.05$). In parental and idelalisib-resistant VL51, MTOR-Ser2448 phosphorylation levels were largely reduced after PQR309 treatment in parental and at less extent also in the resistant cells ($P < 0.05$; Fig. 2F). Changes after anti-IgM stimulation were not evaluated in VL51 because in this cell line there was no increased BCR activation after stimulation (data not shown).

PQR309 inhibits PI3K/mTOR signaling in lymphoma cell lines

PQR309 decreased phosphorylated AKT-Ser473 in unstimulated DLBCL cell lines (2 ABC, 2 GCB) and in 3/4 after stimulation with anti-IgM (Supplementary Fig. S6). Using a cytofluorimetric approach, the PQR309 activity was confirmed in the 2 ABC-DLBCL, and shown in MCL (1/2 unstimulated, 2/2 after stimulation) and CLL (1/1, both conditions) as well (Supplementary Fig. S7). PQR309 also decreased phosphorylation of P70S6K-Thr389 in all the 4 unstimulated cell lines, but not in anti-IgM stimulated cells in which we observed a trend for an increase in phosphorylation levels (Supplementary Fig. S6).

These analyses were extended exposing 8 cell lines to PQR309 or DMSO for 1 and 24 hours and then analyzing the changes in 16 phosphoresidues belonging to 14 proteins involved in the AKT signaling pathway using a protein-array (Supplementary Table S5). PQR309 treatment led to a decrease in the phosphorylation status of 12 residues (RPS6-Ser235/236, PDK1-Ser241, GSK3B-Ser9, AKT1S1-Thr246, P70S6K-Thr421/Ser424, AKT-Thr308, MAPK1-Thr202/Tyr204, RPS6KA1-Thr421/Ser424, BAD-Ser112, PTEN-Ser380, MTOR-Ser2481, PRKAA1/PRKAA2-Thr172). The same six DLBCL and MCL cell lines were then exposed to PQR309 or DMSO for 2 hours, and we measured the changes of 180 phosphoresidues using RPPA (Supplementary Table S6). These analyses confirmed some of the previously obtained results (RPS6-Ser235/Ser236, MAPK1/MAPK3-Thr202/Tyr204) and showed additional phosphorylation changes:

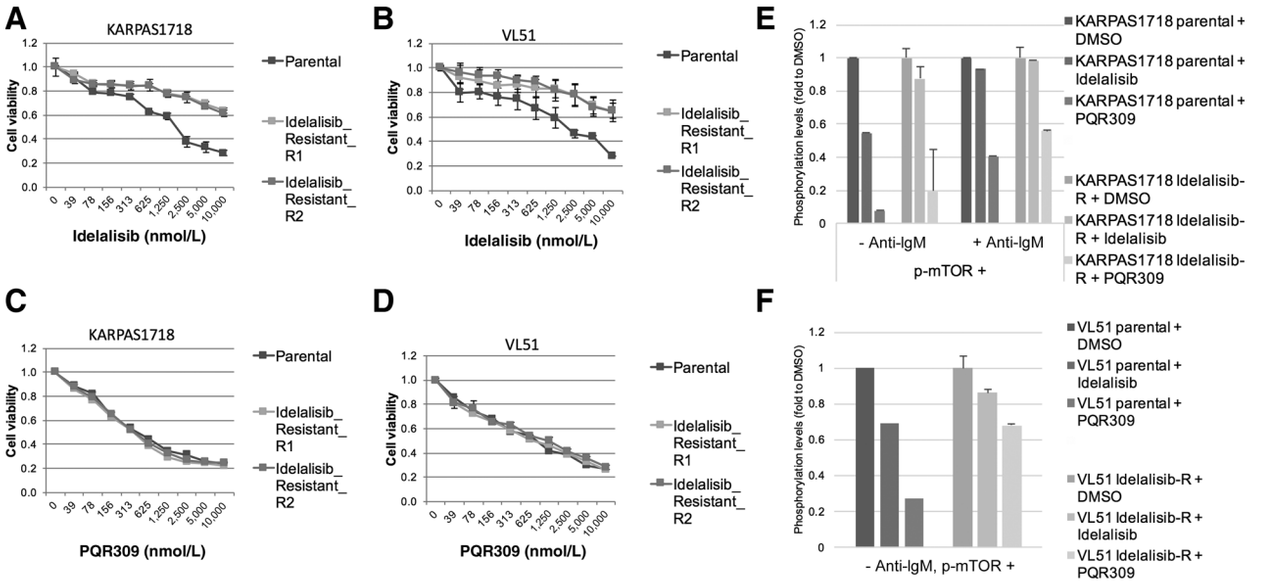

Figure 2.

PQR309 is active in lymphoma cell lines with stable secondary resistance to idelalisib. Antiproliferative activity of idelalisib in KARPAS1718 (**A**) and in VL51 (**B**) parental and in two idelalisib-resistant clones for each. Antiproliferative activity of PQR309 in KARPAS1718 (**C**) and in VL51 (**D**) parental and in two idelalisib-resistant clones each. **E,** Phosphorylation of MTOR-S2448 in KARPAS1718 parental and idelalisib-resistant, treated with DMSO, idelalisib or PQR309 for 16 hours with or without 15 minutes of anti-IgM stimulation (10 μg/μL). KARPAS1718 parental + PQR309 vs. KARPAS1718 parental + DMSO, −anti-IgM, $P < 0.05$; KARPAS1718 parental + PQR309 vs. KARPAS1718 parental + idelalisib, + anti-IgM, $P < 0.05$. **F,** p-MTOR-S2448 activation in VL51 parental and idelalisib-resistant, treated with DMSO, idelalisib or PQR309 for 16 hours. VL51 parental + PQR309 vs. VL51 parental + DMSO, –anti-IgM, $P < 0.05$; VL51 parental + PQR309 vs. VL51 parental + idelalisib, −anti-IgM, $P < 0.05$. Error bars represent the standard deviation on values obtained in two independent experiments.

EIF4G-Ser1108, EIF4EBP1-Thr37 and SMAD3-Ser423/Ser425 were down-phosphorylated, while three phosphoresidues (EIF4EBP1-Thr46, H2AFX-Ser139, PDK1-Ser916) were up-phosphorylated after treatment.

Finally, phosphopeptides were enriched from the cell lysates of the 6 DLBCL and MCL cell lines exposed to PQR309 or DMSO and underwent mass spectrometry analysis. 5,032 peptide assays, including charge states and modifications, were identified, belonging to 4,348 phosphopeptide sequences corresponding to 1,505 protein groups (Supplementary Table S7A). We identified 238 significantly reduced and 242 increased phosphopeptides (Fig. 3; Supplementary Table S7B–S7E), involved in different important pathways, including mRNA processing, apoptosis, PI3K/AKT/mTOR signaling, cell cycle, Myc pathway (Supplementary Table S7F).

Transcriptional signature of PQR309 in DLBCL cell lines

To obtain a global view of the transcriptional changes after PQR309 treatment, we performed GEP on 4 ABC- (RI-1, SU-DHL-2, U2932, TMD8) and 4 GCB-DLBCL (DOHH2, OCI-LY-1, OCI-LY-18, SU-DHL-10), treated with DMSO or with PQR309 (1 μmol/L) for 4, 8, and 12 hours (Fig. 4A, Supplementary Table S8, Supplementary Fig. S8). Transcripts upregulated in ABC-DLBCL (Fig. 4A, Supplementary Table S8, Supplementary Fig. S8) were mainly enriched of genes involved in cell cycle, BCR signaling, and DNA repair (Supplementary Table S8A; Supplementary Fig. S8A). The downregulated transcripts mainly included MYC targets, genes involved in mTOR signaling, unfolded protein response, proteasome, oxidative phosphorylation, glycolysis, and NFKB activation (Supplementary Table S8B;

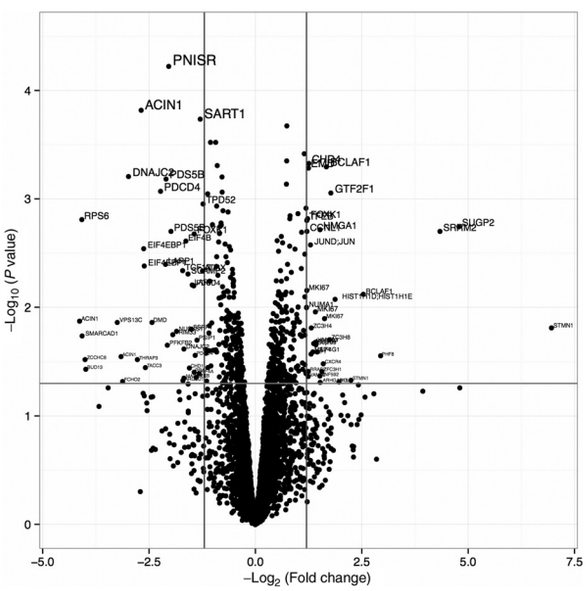

Figure 3.

Phosphopeptide changes after PQR309 treatment. Volcano plot of differentially expressed phosphoproteins after DMSO or 1 μmol/L of PQR309 treatment in six DLBCL and MCL investigated by mass spectrometry. The horizontal line corresponds to $P = 0.05$. The vertical line corresponds to a $\log_2$-fold change = 1.2. X, $\log_2$-fold change. Y, $\log_{10}$ P value.

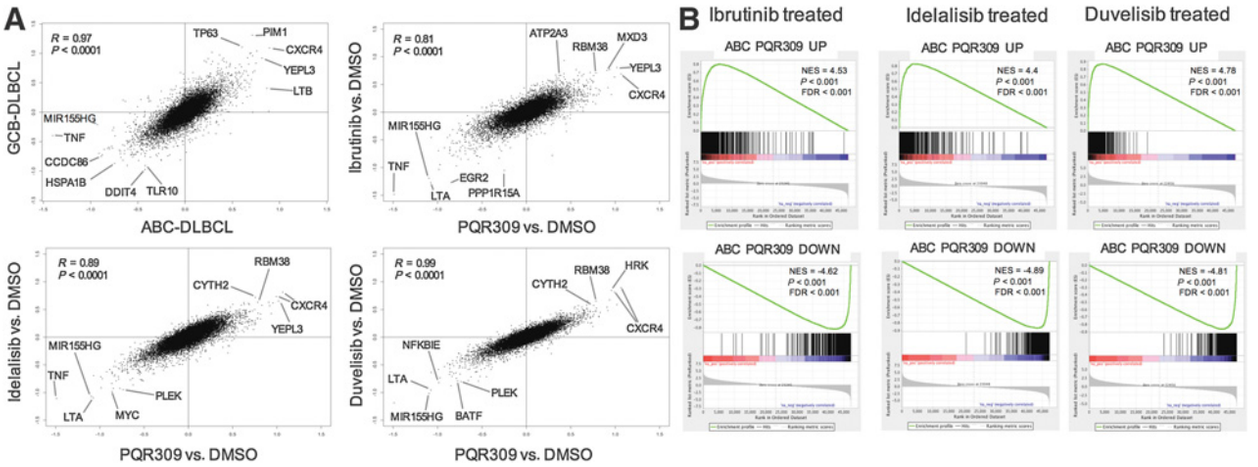

Figure 4.

Gene expression changes after PQR309, ibrutinib, idelalisib, or duvelisib exposure in ABC-DLBCL cell lines. **A,** Scatter plots by $\log_2$-fold gene-expression changes in ABC and GCB DLBCL treated with PQR309, PQR309 + DMSO and ibrutinib + DMSO, PQR309 + DMSO and idelalisib + DMSO, PQR309 + DMSO and duvelisib + DMSO. **B,** GSEA plots for gene-expression signatures obtained in PQR309-treated ABC-DLBCL and then analyzed for their enrichment in ABC-DLBCL exposed to ibrutinib (left), idelalisib (middle), or duvelisib (right). Top, upregulated genes; bottom, downregulated genes. Green line, enrichment score; bars in the middle portion of the plots show where the members of the gene set appear in the ranked list of genes; Positive or negative ranking metric indicates, respectively, correlation or inverse correlation with the profile; NES, normalized enrichment score.

Supplementary Fig. S8B). Similar biologic pathways were affected in treated GCB-DLBCL cells (Supplementary Table S8C and S8D). Indeed, ABC and GCB-DLBCL cell lines exposed to PQR309 presented highly overlapping gene-expression signatures (Supplementary Fig. S9, Fig. 4A). Supplementary Fig. S10 shows validation by real-time PCR, in both GCB and ABC-DLBCL, of selected genes.

Changes in protein phosphorylation and RNA expression contribute differently to PQR309-affected biologic pathways in ABC-DLBCL

To evaluate the contribution of changes in protein phosphorylation and in RNA levels in response to PQR309 in ABC-DLBCL, the list of the differentially phosphorylated proteins (Supplementary Table S7C) was merged with the list of the differentially expressed transcripts (Supplementary Table S8A and S8B). PQR309-induced post-translational changes were more evident on the mRNA metabolism and mTOR pathway, whereas cell-cycle and BCR signaling were affected more via modifications of the expression levels of their components (Supplementary Fig. S11).

Different signaling inhibitors induce similar gene-expression changes

Having observed an upregulation of genes involved in the BCR signaling after exposure to the compound, we assessed whether these changes were specific to PQR309 or shared by other compounds targeting the BCR signaling itself. We treated 4 ABC-DLBCL cell lines (TMD8, RI-1, U2932, and SU-DHL-2) with idelalisib (1 μmol/L), the PI3Kδ/γ inhibitor duvelisib (IPI-145, 1 μmol/L), the BTK inhibitor ibrutinib (500 nmol/L), or PQR309 (1 μmol/L) or DMSO, and we compared the early effects on the transcriptome at 4, 8, and 12 hours (Fig. 4A, Supplementary Table S9). The genome-wide gene-expression changes induced by the four drugs were highly correlated (Fig. 4A). PQR309 was more correlated with the dual PI3Kδ/γ inhibitor than with the single PI3Kδ inhibitor or the BTK inhibitor. PQR309 had a bigger effect on the gene expression of the lymphoma cells than the other drugs, but the same affected genes were largely deregulated, at different degree, also by the other three drugs (Fig. 4A and B). The genes modulated by the other signaling inhibitors were also affected by PQR309 (Supplementary Fig. S12A). There was a positive correlation between exposure to all the individual inhibitors and upregulation of genes coding members of the BCR signaling, such as *CD79B*, *CD79A*, *SYK*, *CBLB*, *ITP3*, *CALM3*, *PLCG1*, *PIK3R1*, *SHC1*, and *SH3KBP1* (Supplementary Fig. S13). *PIK3AP1*, *VAV1*, *BLNK*, and *BTK* were always downregulated.

PQR309 also affected the genes regulated by two other signaling inhibitors in DLBCL cell lines, the dual PI3Kα/δ inhibitor AZD8835 and by the AKT inhibitor AZD5363 (Supplementary Fig. S12B), which appear to exclusively downregulate NFKB or MYC targets, respectively (12).

GEP identifies active PQR309-containing combinations

Because we observed a negative effect of oxidative phosphorylation on the sensitivity of lymphoma cells to PQR309 (Supplementary Fig. S4B; Supplementary Table S3B), we evaluated the combination of the dual PI3K/mTOR inhibitor with metformin, a compound able to inhibit such biologic process (39). All evaluated DLBCL cell lines ($n = 8$) benefited from the combination of PQR309 with metformin.

Because PIM1/PIM2 transcripts appeared upregulated in DLBCL after PQR309 exposure, we evaluated the combination of PQR309 with the PIM kinase inhibitor AZD1208. The combination was beneficial in 12 out of 12 DLBCL (synergistic in five GCB and four ABC, additive in two ABC and one GCB-DLBCL; Supplementary Fig. S14A). Cell-cycle analysis showed an increased arrest in G_0–G_1 for the combination as compared with single treatments (Supplementary Fig. S14B).

Discussion

Here, we have shown that: (i) the novel dual pan-class I PI3K/mTOR inhibitor PQR309 had *in vitro* and *in vivo* antilymphoma activity as single agent and in combination; (ii) specific gene-expression features were associated with sensitivity to the compound; (iii) PQR309 was active in cells with primary or secondary resistance to idelalisib; (iv) modifications of protein phosphorylation and RNA expression differently contribute to PQR309-affected biologic pathways; (v) the gene-expression signatures of PQR309 and of other signaling inhibitors largely overlapped.

PQR309 showed a dose-dependent antitumor activity in most of the analyzed lymphoma cell lines. The median IC_{50} was within the plasma concentration achieved in patients with solid tumors enrolled in the phase I trial (40), and the *in vitro* activity was also confirmed in ABC and GCB-DLBCL xenografts models. Similar to other targeted agents (23, 41), the antitumor activity of PQR309 was mostly cytostatic with a G_1 cell-cycle arrest, as seen with other PI3K and mTOR inhibitors (42, 43).

The antitumor activity of PQR309 was observed also in lymphoma cell lines bearing genetic features associated with a poor clinical outcome and/or chemorefractoriness, such as alterations of *TP53*, *MYC* or *BCL2* genes, or, among DLBCL, with the ABC phenotype or derived from transformed follicular lymphomas. High expression of transcripts involved in PI3K/mTOR pathway, BCR pathway, kinase regulation and immune system was associated with higher sensitivity to PQR309. The transcription levels of genes coding for PI3Kδ and the regulatory subunits p85α and p85β were prominent in cell lines highly sensitive to PQR309, while the opposite was true for transcripts encoding the catalytic subunits of PI3Kγ and PI3Kα and the PI3Kγ adaptor subunit p84. Moreover, a small panel of genes appeared associated with sensitivity to PQR309, both using a microarray-based approach and target RNA-Seq technique, and could be further validated in the on-going and in the future trials with PQR309 or other dual PI3K-mTOR inhibitors.

PQR309 was active also in cell lines with primary or secondary resistance to idelalisib. Cell lines sensitive to both idelalisib and PQR309 were characterized by high expression levels of genes involved in the PI3K/mTOR pathway, IFN and cytokine/chemokine signaling, including transcripts such *CD86*, *IRF7* and *IRF9*, *CCL3* and *CCL4*, also in accordance with the literature (44). Cell lines sensitive only to PQR309 had high expression of cell cycle and amino acid metabolism genes, comprising the oncogenic transcription factor SOX4, a known component of the PTEN/PI3K/AKT pathway. Reflecting the different specificity of idelalisib and PQR309 towards the PI3K isoforms, the dual sensitive cell lines had higher levels of PI3Kδ while PI3Kα, PI3Kβ and PI3Kγ were more expressed in the group responding only to PQR309. Interestingly, cell lines resistant to idelalisib still responded to PQR309 decreasing the levels of MTOR phosphorylation.

PQR309 was combined with agents targeting important biological pathways and showed synergism when combined in various DLBCL or MCL models, including some derived from double hit lymphomas. Most benefit was obtained combining the novel compound with venetoclax, ibrutinib, panobinostat and lenalidomide, agents all in the clinical setting, as also confirmed with experiments using xenografts and/or primary cells, and with the BET degrader ARV-825, which is still an experimental agent. Despite the limitation given by the lack of experiments on patient-derived xenografts, our results are in agreement with what was reported for other PI3K and/or mTOR inhibitors (12, 23, 41, 45) and support the clinical exploration of these combinations.

High expressions of genes coding proteins involved in the oxidative phosphorylation process were associated with lower sensitivity to PQR309. Interestingly, the addition of metformin, an antidiabetic drug known to affect oxidative phosphorylation (39), to PQR309 resulted in a synergism in eight out of eight DLBCL cell lines, suggesting that the combination is worth of further investigations.

PQR309 exposure affected transcripts and proteins involved in fundamental pathways and signaling cascades: PI3K/AKT/mTOR pathway, BCR signaling, NFKB pathway, mRNA processing, apoptosis, cell cycle, Myc pathway, MAPK/RAS signaling, and glycolysis. Most of the pathways were largely modulated via both RNA and protein phosphorylation changes. However, the latter played a bigger role on the mRNA metabolism and mTOR pathway, reflecting the direct mechanism of action of PQR309, whereas changes in cell cycle and BCR signaling appeared more driven at RNA level. Among individual genes affected by PQR309, it is worth to mention a few genes with a role in lymphomas. *YPEL3*, *TP63* and *HRK* were upregulated. *HSPA8* and *HSPA1B* (Hsp70), *MIR155HG*, *CCDC86* (Cyclon) and *PAK1IP1* were downregulated. Ki67, HMGA1 and JUND had a reduction in their phosphorylation, whereas the opposite was seen for NFKB1 and IKZF1. CXCR4 appeared regulated at both transcriptional and post-translational level, and could represent a possible mechanism of adaptive resistance. PQR309 exposure induced the upregulation of both *PIM1* and *PIM2*, kinases involved in lymphomagenesis and potential therapeutic targets. We combined PQR309 with the PIM inhibitor AZD1208 (46) with beneficial effect of the combination with an increased G_0–G_1 cell-cycle arrest.

To have a better insight on the early changes induced by PQR309 in comparison with other signaling inhibitors, we performed GEP on ABC-DLBCL cell lines exposed to PQR309, idelalisib, duvelisib, and ibrutinib. All the compounds presented very similar effects, in line with what data reported in normal B cells after genetic silencing of BTK and PI3K (47). *CXCR4*, *BRD8*, *CDKN2C*, *YPEL3*, *HRK* were among the most recurrently upregulated, whereas *LTA*, *TNF*, *MIR155HG*, *NFKBIE*, *SGK1*, *LMO2*, *CCL3* were recurrently downregulated. All the compounds induced an early upregulation of genes coding members of the BCR signaling possibly reflecting a feedback loop or an adaptive mechanism, which, however, did not negatively impact the antiproliferative activity of the compounds possibly due to the continuous exposure.

Phase I studies have been completed with PQR309 as single agent in patients with solid tumors and in lymphomas (40, 48), and the agent is now in phase II for different indications, including for patients with relapsed and refractory lymphoma patients (NCT02249429, NCT03127020), with relapsed and refractory primary central nervous system lymphoma (PCNSL; NCT02669511, NCT03120000).

In conclusion, the novel dual PI3K/mTOR inhibitor PQR309 presented promising activity as single agent and in combination. GEP and mass spectrometry allowed the identification of biologic features associated with drug sensitivity and with its mechanisms of action. Different signaling inhibitors appeared to induce largely shared early changes in the expression profiles of lymphoma cells.

Disclosure of Potential Conflicts of Interest

M.P. Wymann is an employee of and has ownership interests (including patents) at PIQUR Therapeutics AG. A. Wicki is a consultant/advisory board member for Actelion/Indorsia. F. Bertoni reports receiving commercial research grants from PIQUR. No potential conflicts of interest were disclosed by the other authors.

Authors' Contributions

Conception and design: C. Tarantelli, E. Gaudio, P. Hillmann, L. Carrassa, F. Beaufils, M. Broggini, M.P. Wymann, A. Wicki, V. Cmiljanovic, D. Fabbro, F. Bertoni
Development of methodology: C. Tarantelli, L. Carrassa, F. Beaufils, D. Rageot, A. Sele, M.P. Wymann, A. Wicki
Acquisition of data (provided animals, acquired and managed patients, provided facilities, etc.): C. Tarantelli, A.J. Arribas, P. Hillmann, A. Rinaldi, E. Bernasconi, F. Guidetti, R. Bordone Pittau, F. Beaufils, R. Ritschard, F.M. Rossi, A. Zucchetto, V. Gattei, G. Stussi, M. Broggini, A. Wicki, D. Fabbro, F. Bertoni
Analysis and interpretation of data (e.g., statistical analysis, biostatistics, computational analysis): C. Tarantelli, E. Gaudio, A.J. Arribas, I. Kwee, L. Cascione, E. Bernasconi, R. Ritschard, B. Dossena, M. Taborelli, V. Gattei, A. Wicki, D. Fabbro, F. Bertoni
Writing, review, and/or revision of the manuscript: C. Tarantelli, A.J. Arribas, P. Hillmann, D. Rossi, A. Stathis, G. Stussi, M. Broggini, M.P. Wymann, A. Wicki, E. Zucca, V. Cmiljanovic, F. Bertoni
Administrative, technical, or material support (i.e., reporting or organizing data, constructing databases): C. Tarantelli, M.P. Wymann, D. Fabbro, F. Bertoni
Study supervision: V. Cmiljanovic, D. Fabbro, F. Bertoni
Other (performed experiments): F. Spriano
Other (compound design): D. Rageot
Other (compound design, SAR of PQR309): A. Sele

Acknowledgments

Partially supported by institutional research funds from PIQUR AG; the Barletta and Gelu Foundations; Swiss National Science Foundation (SNSF) grant 31003A_163232 (to F. Bertoni); Swiss Commission for Technology and Innovation (CTI) PFLS-LS grants 14032.1, 15811.2, and 17241.1; SNSF grants 310030_153211 and 316030_133860 (to M.P. Wymann); the Italian Association for Cancer Research (L. Carrassa and M. Broggini); Mu.Ta.Lig. COST Action CA15135 (to E. Gaudio); GR-2011-02346826 (to A. Zucchetto); and AIRC IG-17622 (to V. Gattei).

The costs of publication of this article were defrayed in part by the payment of page charges. This article must therefore be hereby marked *advertisement* in accordance with 18 U.S.C. Section 1734 solely to indicate this fact.

Received April 11, 2017; revised September 18, 2017; accepted October 20, 2017; published OnlineFirst October 24, 2017.

References

1. Liu P, Cheng H, Roberts TM, Zhao JJ. Targeting the phosphoinositide 3-kinase pathway in cancer. Nat Rev Drug Discov 2009;8:627–44.
2. Thorpe LM, Yuzugullu H, Zhao JJ. PI3K in cancer: divergent roles of isoforms, modes of activation and therapeutic targeting. Nat Rev Cancer 2015;15:7–24.
3. Blachly JS, Baiocchi RA. Targeting PI3-kinase (PI3K), AKT, and mTOR axis in lymphoma. Br J Haematol 2014;167:19–32.
4. Iyengar S, Clear A, Bodor C, Maharaj L, Lee A, Calaminici M, et al. P110alpha-mediated constitutive PI3K signaling limits the efficacy of p110delta-selective inhibition in mantle cell lymphoma, particularly with multiple relapse. Blood 2013;121:2274–84.
5. Psyrri A, Papageorgiou S, Liakata E, Scorilas A, Rontogianni D, Kontos CK, et al. Phosphatidylinositol 3′-kinase catalytic subunit alpha gene amplification contributes to the pathogenesis of mantle cell lymphoma. Clin Cancer Res 2009;15:5724–32.
6. Abubaker J, Bavi PP, Al-Harbi S, Siraj AK, Al-Dayel F, Uddin S, et al. PIK3CA mutations are mutually exclusive with PTEN loss in diffuse large B-cell lymphoma. Leukemia 2007;21:2368–70.
7. Pfeifer M, Grau M, Lenze D, Wenzel SS, Wolf A, Wollert-Wulf B, et al. PTEN loss defines a PI3K/AKT pathway-dependent germinal center subtype of diffuse large B-cell lymphoma. Proc Natl Acad Sci U S A 2013;110: 12420–5.
8. Yahiaoui OI, Nunes JA, Castanier C, Devillier R, Broussais F, Fabre AJ, et al. Constitutive AKT activation in follicular lymphoma. BMC Cancer 2014; 14:565.
9. Avivi I, Goy A. Refining the mantle cell lymphoma paradigm: impact of novel therapies on current practice. Clin Cancer Res 2015;21: 3853–61.
10. Cheah CY, Fowler NH. Idelalisib in the management of lymphoma. Blood 2016;128:331–6.
11. Miller BW, Przepiorka D, de Claro RA, Lee K, Nie L, Simpson N, et al. FDA approval: idelalisib monotherapy for the treatment of patients with follicular lymphoma and small lymphocytic lymphoma. Clin Cancer Res 2015;21:1525–9.
12. Erdmann T, Klener P, Lynch JT, Grau M, Vockova P, Molinsky J, et al. Sensitivity to PI3K and AKT inhibitors is mediated by divergent molecular mechanisms in subtypes of DLBCL. Blood 2017;130:310–22.
13. Gaudio E, Tarantelli C, Spriano F, Bernasconi E, Targa A, Dirnhofer S, et al. The novel BTK and PI3K-delta inhibitors acalabrutinib (ACP-196) and ACP-319 show activity in pre-clinical B-cell lymphoma models. Eur J Cancer 2016;69:S39–S40.
14. Dong S, Guinn D, Dubovsky JA, Zhong Y, Lehman A, Kutok J, et al. IPI-145 antagonizes intrinsic and extrinsic survival signals in chronic lymphocytic leukemia cells. Blood 2014;124:3583–6.
15. Paul J, Soujon M, Wengner AM, Zitzmann-Kolbe S, Sturz A, Haike K, et al. Simultaneous inhibition of PI3Kd and PI3Ka induces ABC-DLBCL regression by blocking BCR-dependent and -independent activation of NF-kB and AKT. Cancer Cell 2017;31:64–78.
16. Serra V, Markman B, Scaltriti M, Eichhorn PJ, Valero V, Guzman M, et al. NVP-BEZ235, a dual PI3K/mTOR inhibitor, prevents PI3K signaling and inhibits the growth of cancer cells with activating PI3K mutations. Cancer Res 2008;68:8022–30.
17. O'Reilly KE, Rojo F, She QB, Solit D, Mills GB, Smith D, et al. mTOR inhibition induces upstream receptor tyrosine kinase signaling and activates Akt. Cancer Res 2006;66:1500–8.
18. Beaufils F, Cmiljanovic N, Cmiljanovic V, Bohnacker T, Melone A, Marone R, et al. 5-(4,6-Dimorpholino-1,3,5-triazin-2-yl)-4-(trifluoromethyl)pyridin-2-amine (PQR309), a potent, brain-penetrant, orally bioavailable, pan-class I PI3K/mTOR inhibitor as clinical candidate in oncology. J Med Chem 2017;60:7524–38.
19. Bohnacker T, Prota AE, Beaufils F, Burke JE, Melone A, Inglis AJ, et al. Deconvolution of Buparlisib's mechanism of action defines specific PI3K and tubulin inhibitors for therapeutic intervention. Nat Commun 2017;8:14683.
20. Salphati L, Heffron TP, Alicke B, Nishimura M, Barck K, Carano RA, et al. Targeting the PI3K pathway in the brain–efficacy of a PI3K inhibitor optimized to cross the blood-brain barrier. Clin Cancer Res 2012; 18:6239–48.
21. Chila R, Basana A, Lupi M, Guffanti F, Gaudio E, Rinaldi A, et al. Combined inhibition of Chk1 and Wee1 as a new therapeutic strategy for mantle cell lymphoma. Oncotarget 2015;6:3394–408.
22. Mensah AA, Kwee I, Gaudio E, Rinaldi A, Ponzoni M, Cascione L, et al. Novel HDAC inhibitors exhibit pre-clinical efficacy in lymphoma models and point to the importance of CDKN1A expression levels in mediating their anti-tumor response. Oncotarget 2015;6: 5059–71.
23. Boi M, Gaudio E, Bonetti P, Kwee I, Bernasconi E, Tarantelli C, et al. The BET bromodomain inhibitor OTX015 affects pathogenetic pathways in preclinical B-cell tumor models and synergizes with targeted drugs. Clin Cancer Res 2015;21:1628–38.
24. Chou TC. Drug combination studies and their synergy quantification using the Chou-Talalay method. Cancer Res 2010;70:440–6.

25. Boi M, Rinaldi A, Kwee I, Bonetti P, Todaro M, Tabbo F, et al. PRDM1/BLIMP1 is commonly inactivated in anaplastic large T-cell lymphoma. Blood 2013;122:2683–93.
26. Olsen JV, Blagoev B, Gnad F, Macek B, Kumar C, Mortensen P, et al. Global, in vivo, and site-specific phosphorylation dynamics in signaling networks. Cell 2006;127:635–48.
27. Cox J, Mann M. MaxQuant enables high peptide identification rates, individualized p.p.b.-range mass accuracies and proteome-wide protein quantification. Nat Biotech 2008;26:1367–72.
28. Bonetti P, Testoni M, Scandurra M, Ponzoni M, Piva R, Mensah AA, et al. Deregulation of ETS1 and FLI1 contributes to the pathogenesis of diffuse large B-cell lymphoma. Blood 2013;122:2233–41.
29. Arloth J, Bader DM, Röh S, Altmann A. Re-annotator: annotation pipeline for microarray probe sequences. PLoS One 2015;10:e0139516.
30. Reinholz MM, Thompson DM, Botros I, Rounseville M, Roche PC. Abstract 1383: NGS-based measurement of gene expression of 2560 oncology-related biomarkers in formalin-fixed, paraffin-embedded (FFPE) tissues. Cancer Res 2016;76:1383-.
31. Smyth GK. Linear models and empirical Bayes methods for assessing differential expression in microarray experiments. Stat Appl Genet Mol Biol 2004;3:Article3.
32. Subramanian A, Tamayo P, Mootha VK, Mukherjee S, Ebert BL, Gillette MA, et al. Gene set enrichment analysis: a knowledge-based approach for interpreting genome-wide expression profiles. Proc Natl Acad Sci U S A 2005;102:15545–50.
33. Shaffer AL, Wright G, Yang L, Powell J, Ngo V, Lamy L, et al. A library of gene expression signatures to illuminate normal and pathological lymphoid biology. Immunol Rev 2006;210:67–85.
34. Rainer J, Sanchez-Cabo F, Stocker G, Sturn A, Trajanoski Z. CARMAweb: comprehensive R- and bioconductor-based web service for microarray data analysis. Nucleic Acids Res 2006;34:W498–503.
35. Tarazona S, Furio-Tari P, Turra D, Pietro AD, Nueda MJ, Ferrer A, et al. Data quality aware analysis of differential expression in RNA-seq with NOISeq R/Bioc package. Nucleic Acids Res 2015;43:e140.
36. Dolly SO, Wagner AJ, Bendell JC, Kindler HL, Krug LM, Seiwert TY, et al. Phase I study of apitolisib (GDC-0980), dual phosphatidylinositol-3-kinase and mammalian target of rapamycin kinase inhibitor, in patients with advanced solid tumors. Clin Cancer Res 2016;22:2874–84.
37. Kahl BS, Spurgeon SE, Furman RR, Flinn IW, Coutre SE, Brown JR, et al. A phase 1 study of the PI3Kdelta inhibitor idelalisib in patients with relapsed/refractory mantle cell lymphoma (MCL). Blood 2014;123:3398–405.
38. Arribas AJ, Gaudio E, Rinaldi A, Cascione L, Tarantelli C, Kwee I, et al. Development of preclinical models of secondary resistance to idelalisib in splenic marginal zone lymphoma (SMZL). Hematol Oncol 2017; 35 (suppl. S2):254.
39. Bridges HR, Jones AJ, Pollak MN, Hirst J. Effects of metformin and other biguanides on oxidative phosphorylation in mitochondria. Biochem J 2014;462:475–87.
40. Kristeleit RS, Brown NF, Hess D, Joerger M, Von Moos R, Rodón J, et al. Abstract 2592: A phase 1 first-in-human (FIH) dose-escalation (DE) study of the oral dual PI3K/mTOR inhibitor PQR309 in patients (pts) with advanced solid tumors: Final DE results. J Clin Oncol;33:15s, 2015 (suppl; abstract 2592).
41. Ezell SA, Mayo M, Bihani T, Tepsuporn S, Wang S, Passino M, et al. Synergistic induction of apoptosis by combination of BTK and dual mTORC1/2 inhibitors in diffuse large B cell lymphoma. Oncotarget 2014;5:4990–5001.
42. Meadows SA, Vega F, Kashishian A, Johnson D, Diehl V, Miller LL, et al. PI3Kdelta inhibitor, GS-1101 (CAL-101), attenuates pathway signaling, induces apoptosis, and overcomes signals from the microenvironment in cellular models of Hodgkin lymphoma. Blood 2012;119:1897–900.
43. Bohnacker T, Beaufils F, Prota AE, Burke JE, Melone A, Inglis AJ, et al. Abstract 671: BKM120-mediated G2 arrest: Structural and functional segregation of off-target action and PI3K inhibition. Cancer Res 2015;75:671.
44. Takahashi K, Sivina M, Hoellenriegel J, Oki Y, Hagemeister FB, Fayad L, et al. CCL3 and CCL4 are biomarkers for B cell receptor pathway activation and prognostic serum markers in diffuse large B cell lymphoma. Br J Haematol 2015;171:726–35.
45. Mathews Griner LA, Guha R, Shinn P, Young RM, Keller JM, Liu D, et al. High-throughput combinatorial screening identifies drugs that cooperate with ibrutinib to kill activated B-cell-like diffuse large B-cell lymphoma cells. Proc Natl Acad Sci U S A 2014;111:2349–54.
46. Keeton EK, McEachern K, Dillman KS, Palakurthi S, Cao Y, Grondine MR, et al. AZD1208, a potent and selective pan-Pim kinase inhibitor, demonstrates efficacy in preclinical models of acute myeloid leukemia. Blood 2014;123:905–13.
47. Fruman DA, Ferl GZ, An SS, Donahue AC, Satterthwaite AB, Witte ON. Phosphoinositide 3-kinase and Bruton's tyrosine kinase regulate overlapping sets of genes in B lymphocytes. Proc Natl Acad Sci U S A 2002;99:359–64.
48. Collins GP, Popat R, Stathis A, Krasniqi F, Eyre TA, Ng CH, et al. A dose-escalation (DE) study with expansion evaluating safety, pharmacokinetics and efficacy of the novel, balanced PI3K/mTOR inhibitor PQR309 in patients with relapsed or refractory lymphoma. Blood 2016;128:5893-.